Accepted Manuscript

Optical properties of wine pigments: theoretical guidelines with new methodological perspectives

Patrick Trouillas, Florent Di Meo, Johannes Gierschner, Mathieu Linares, Juan Carlos Sancho-García, Michal Otyepka

PII: S0040-4020(14)01485-9

DOI: 10.1016/j.tet.2014.10.046

Reference: TET 26116

To appear in: *Tetrahedron*

Received Date: 9 June 2014

Revised Date: 7 October 2014

Accepted Date: 20 October 2014

Please cite this article as: Trouillas P, Di Meo F, Gierschner J, Linares M, Sancho-García JC, Otyepka M, Optical properties of wine pigments: theoretical guidelines with new methodological perspectives, *Tetrahedron* (2014), doi: 10.1016/j.tet.2014.10.046.

Optical properties of wine pigments: theoretical guidelines with new methodological perspectives

Patrick Trouillas,[a,b,*] Florent Di Meo,[c] Johannes Gierschner,[d] Mathieu Linares,[c] Juan Carlos Sancho-García,[e] and Michal Otyepka[b]

[a]INSERM S850, Université de Limoges, 2 rue du Dr Marcland, F-87025 Limoges, France

[b]Regional Centre of Advanced Technologies and Materials, Department of Physical Chemistry, Faculty of Science, Palacký University of Olomouc, tr. 17. listopadu 12, 771 46 Olomouc, Czech Republic

[c]Department of Physics, Chemistry and Biology (IFM), Linköping University, SE-58183 Linköping, Sweden

[d]Madrid Institute for Advanced Studies - IMDEA Nanoscience, C/ Faraday 9, Ciudad Universitaria de Cantoblanco, E-28049 Madrid, Spain

[e]Departamento de Química Física, Universidad de Alicante, Apartado de Correos 99, E-03080 Alicante, Spain

Keywords: WINE PIGMENTS; ANTHOCYANINS; QUANTUM CHEMISTRY; DISPERSIVE&RSH (TD)-DFT; COPIGMENTATION; MOLECULAR DYNAMICS

Graphical Abstract

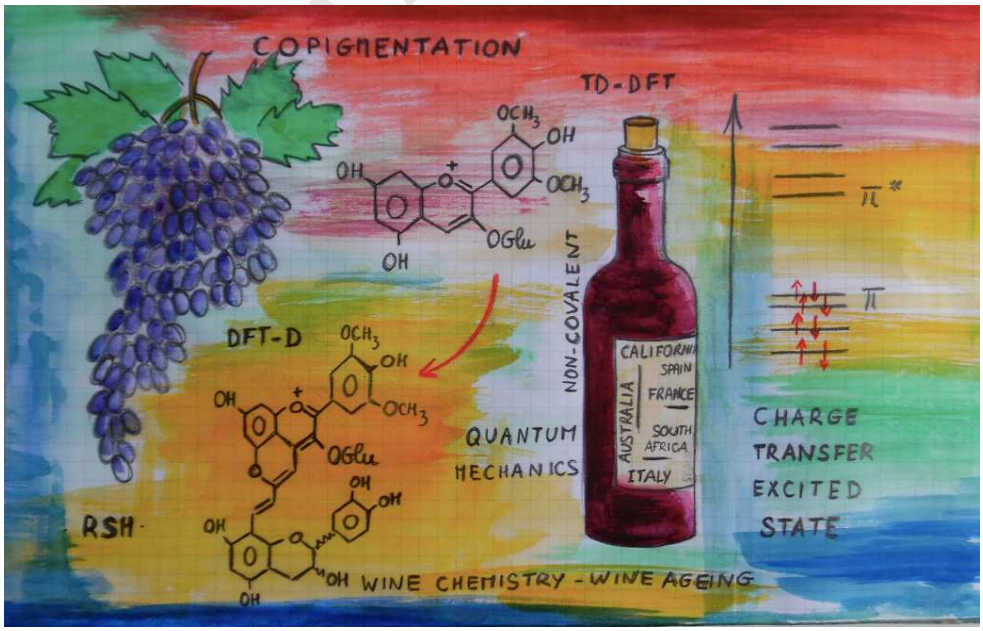

* Corresponding author. Tel. : +33 555 435 927, e-mail address: patrick.trouillas@unilim.fr

Contents

Abstract

Wine pigmentation results from the complex chemistry of anthocyanins. Their flavylium cation form is stabilized either by chemical transformation occurring during wine aging (e.g., pyranoanthocyanin formation), or by the formation of non-covalent complexes with (phenolic) copigments.

Molecular modelling (quantum mechanics and molecular dynamics) is more and more adapted to understand wine chemistry and pigmentation. The constant developments of theoretical methodologies might get non-specialists easily lost. This manuscript is a review of the theoretical studies dedicated to the field of wine pigments, showing conformational analysis, energetics of the various forms, pigment/copigment (non-)covalent association and charge transfer excited states. QM/MM calculations are newly performed here, which improve solvent description. The conclusion is a comprehensive guideline for an accurate prediction of light absorption by wine pigments and all related supramolecular processes.

1. Introduction

Wine pigmentation has been the subject of intense research over the last twenty years, revealing a rather sophisticated wine chemistry regarding the complexity of dye composition and molecular electronic parameters that influence the color of the wine.[1-4] The most important group of phenolic wine pigments* are anthocyanin derivatives. Wine anthocyanins are mainly derived from five aglycones (anthocyanidins), namely cyanidin, peonidin, petunidin, delphinidin and malvidin (Figure 1). They are usually represented in their flavylium cation form (AH^+), which is mainly responsible for the red color of the wine. However, this form is only favored at pH < 2, whereas under ambient wine conditions, at a pH of about 3.6, an acid-base equilibrium exists (Figure 1). Under the latter conditions, the corresponding quinonoidal bases (i.e., neutral purple A, anionic blue A^- and possibly dianionic A^{2-}) coexist with their hydrated forms, i.e., colorless hemiketals (AOH), in equilibrium with the corresponding tautomeric chalcones (yellowish hue). Accordingly, at wine pH, colorless anthocyanin derivatives should prevail (75-95%),[1] which does not sufficiently explain the actual red wine color. In fact, various natural processes stabilize the AH^+ form, and thus red (or close to red) colors. These processes can essentially be classed as chemical transformations and/or the formation of non-covalently stacked complexes.

* We use the term 'pigments' as commonly used in life sciences to refer to both soluble and non-soluble natural organic colorants in contrast to chemistry, where in principle a distinction between 'dye' (soluble) and 'pigment' (non-soluble) is made.

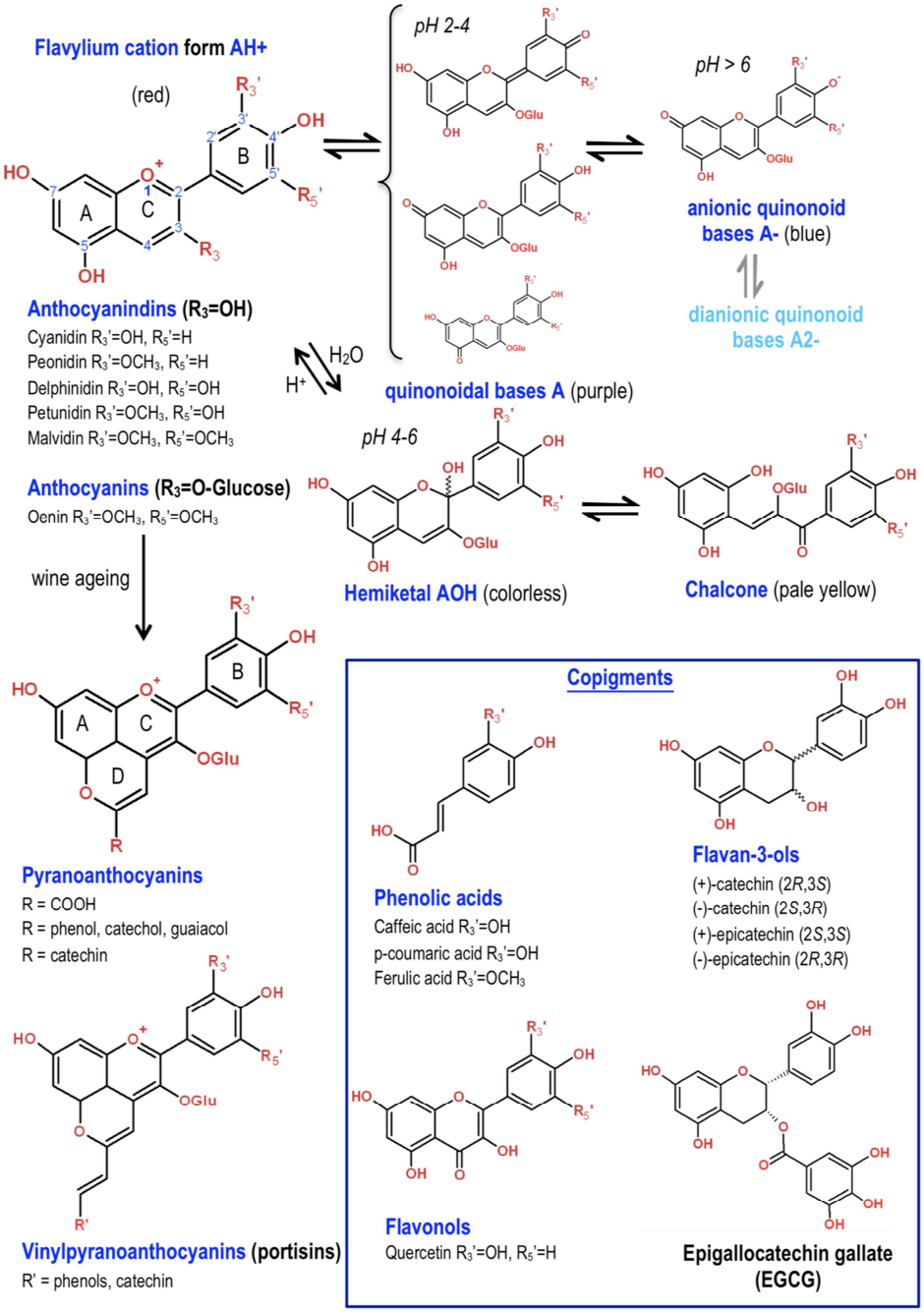

Figure 1: Chemical structures of the most important wine pigments and copigments. The pH and colors are indicative as they depend on substituents.

Chemical transformations include[2-3] the formation of flavanol-anthocyanin adducts (with or without CH_3-CH bridges originating from EtOH); anthocyanin dimers and related polymers, pyranoanthocyanins (e.g., vitisins A&B, oxovitisins); pyranoanthocyanin-phenols; pyranoanthocyanin-flavanols; and the more recently discovered vinylpyranoanthocyanins, e.g., the bluish (at acidic pH) vinylpyranoanthocyanin-flavanol portisin (Figure 1).[5-8] Most of these pigments are synthesized during wine storage and ageing. They have extended π-conjugated systems, in which the flavylium cation form is stabilized, which therefore exhibit visible colors (red to orange hue).[9-10]

The other process that stabilizes the flavylium cation form at wine pH is the formation of non-covalent complexes. As a π-conjugated moiety, anthocyanidin has long been considered as a candidate for copigmentation, favoring π-stacking.[11-14] The flavylium cations of anthocyanin and pyranoanthocyanin derivatives associate with various copigments to different degrees (mainly with flavonols, flavan-3-ols and phenolic acids, see Figure 1).[15-16] In red wine, copigmentation shifts the color bathochromically toward purple and shows a hyperchromic effect, which can be conveniently followed by UV/Vis absorption spectroscopy. Metal ions may also participate in such copigmentation association.

A full understanding of the wine chemistry and supramolecular arrangements (mainly related to copigmentation) responsible for the final pigmentation is of particular interest for wine makers. Because of its complexity, experimental quantification of wine phenolic composition together with related physicochemical properties is still challenging.[1, 17-18] In the near future, molecular modeling might enhance our understanding of the physical-chemical properties of such complex systems. Over the last few decades, molecular dynamics (MD) and quantum chemistry (QC) techniques have significantly developed and appear suitable for evaluating conformational, stacking, chemical and optical features of wine polyphenols.

The present article intends to provide a comprehensive and insightful review of techniques for calculating wine pigment properties, showing the most advanced developments in the field. After a brief review of the early calculations of wine pigments with semi-empirical methods (section 2), we discuss the use of (time-dependent) density functional theory ((TD)-DFT) for calculating molecular geometries (section 3.1), chemical reactivity (section 3.2) and optical properties (section 3.3) of anthocyanin derivatives. Recent theoretical studies of the copigmentation process are then discussed, focusing mainly on conformational analysis (section 4.1), evaluation of association energies with various formalisms to account for dispersion interactions (section 4.2) and optical properties highlighting the importance of an adequate description of charge transfer (CT) contributions (section 4.3). Section 5 demonstrates how molecular orbital (MO) analysis allows a detailed insight into the pigmentation process. Proper accounting for the environment, mainly solvent effects, is a critical challenge in molecular modeling. Section 6.1 discusses the use of implicit solvents via the polarizable continuum model (PCM) for predicting wine pigmentation, where it is stressed that refinements must be carefully considered for an accurate description of excited states (ES). Section 6.2 proposes new refinements based on QM/MM with a fully self-consistent polarizable embedding (PE) scheme and a series of calculations for anthocyanin and non-covalent anthocyanin-flavonol prototypes newly performed for the current work. Finally, the conclusion (section 7) proposes comprehensive guidelines for the accurate prediction of light absorption by wine pigments and all related supramolecular processes.

2. Early history of wine pigment calculations

In 1965, G. V. Boyd and N. Singer[19] reported Hückel molecular orbital (HMO) calculations for 65 pyrylium salts correlating the calculated state energies (Δm)[*] and experimental absorption maxima energies. The authors pointed out that the HMO assumption of coplanar systems might be problematic and stressed the need for parameterization to properly account for π-conjugation in these systems. In a later study, they emphasized problems of theoretical methods for dealing with the flavylium series, even when including configuration interaction within the newly developed semi-empirical schemes, like the Pariser-Parr-Pople (PPP) technique.[20]

In the 1990s, with the emergence of more powerful semi-empirical techniques that could be handled by the steadily improving computational power, a few studies focused on the chemical and optical properties of anthocyanidins, in which e.g. the coplanarity was again under debate[†],[24,25] highlighting that even in the presence of OH groups in the B-ring, the conjugation between the B- and C-rings remains too small with the semi-empirical AM1 method. Despite this incorrect description of π-conjugation, AM1 succeeded in rationalizing some structure-property relationships, such as *i)* OH substitution in the B-ring, which induces absorption at longer wavelength (red shift), and *ii)* inductive substitution effects, which increase the effective π-conjugation between the B- and C-rings.[25-26]

With the rise in (TD)-DFT methods at the end of the 1990s, which provide a reasonable description of π-conjugation in medium-sized systems (vide infra) and can nowadays be performed at low computational costs, the pioneering use of semi-empirical methods have lost its general importance, except the INDO method as parameterized by Zerner for spectroscopic

[*] Δm is defined in the Hückel formalism as the difference in m_k between both energy levels involved in the $\pi \rightarrow \pi^*$ electronic transition. Within the Hückel formalism and for unsaturated hydrocarbon chains, m_k appears in the energy of state k as $E_k = \alpha + m_k \beta$, α and β being the Coulomb integral related to p-orbitals of carbons and the carbon-carbon bond integral, respectively.

[†] HF/6-31G*//HF/3-21G also result from the underestimation of π-delocalization within these schemes,[21] which is (as we now know[22]) incorrect. This work showed rather good agreement with X-ray diffraction crystal structure analysis.[23] However, torsional angles in conjugated organic compounds are known to easily adapt to the external constraints within the crystal. Thus, comparisons to gas phase and solvent calculations are not necessarily valid.

applications (ZINDO).[27] This method, now often based on DFT-optimized geometries, remains popular due to its size consistency with increasing conjugation length[28-29] and ability to handle large molecular clusters.

3. Calculation of molecular properties

The last decade has highlighted the capacity of DFT (mainly with hybrid functionals) to predict various properties of polyphenols, including antioxidant action,[30-39] metal complexation,[40-43] reactivity,[21, 44] and optical properties.[45-47] DFT studies* on anthocyanins have enabled accurate evaluation of conformational, thermodynamic and spectroscopic features (see sections 3.1, 3.2 and 3.3, respectively).

3.1. Geometrical issues

Already discussed from semi-empirical calculations (vide supra), the planarity of anthocyanins has been the subject of intense discussions.[22,48,49,50,51] An accurate QC methodology was required as the comparison to X-ray analyses is rather limited since crystal packing may induce severe constraints that do not exist in solution. To sum up and conclude from all theoretical studies, anthocyanidins are planar systems but the B-ring can almost freely rotate, giving rise to a broad distribution of conformers under ambient conditions. The presence of bulky chemical groups, such sugar moieties in anthocyanins (e.g., at C3, see Figure 1), can twist the B-ring and constrain the free torsion. Within the DFT framework, both the functional and basis set have to be carefully chosen to accurately describe π-conjugation, mainly when aiming not only at conformation analysis but also at a further

* One of the most important issues in DFT is careful choice of the functional according to the molecular system and physical property under study. The use of hybrid functionals (i.e., B3LYP or B3P86) is currently the preferred way to achieve a decent compromise between accuracy and computational cost. The way is which the HF- (or exact-like) exchange is adequately combined with an exchange density functional compensates for the underestimation by the former of the strength of conjugation; the use of a pure density functional is thus no longer recommended.

comprehensive description of MOs and electronic transitions, which characterize the optical properties. For anthocyanin derivatives, hybrid functionals can adequately describe the conformational space (see the previous footnote), and larger basis set (easily handled with the current computational power) are recommended to avoid errors in the description of the torsional potential. Finally, solvent effects must be taken into account, e.g., by using polarizable continuum models (PCM). Even if it is somewhat challenging to reach accuracy, accounting for solvent effects in the calculation is mandatory, especially when dealing with charged species, such as AH^+. This issue will be detailed in section 6.

3.2. pKa and stabilizing relative energies

Another important theoretical issue in wine chemistry is the rationalization of the acid-base equilibria of anthocyanins, which requires a good theoretical description of both neutral and (various) charged states. To calculate the thermodynamics accurately, hybrid functionals are recommended,[34] whereas pure DFT functionals systematically fail.

Using a classical thermodynamic scheme, pKa were calculated from standard free energies with the mPWP1PW91 functional (including PCM) for different flavylium salts, with a reasonable agreement between experimental and theoretical data.[52] The pKas of flavylium salts were also reasonably predicted based on QSPR (quantitative structure–property relationships) and molecular and topological descriptors.[53] Whereas experiments provide macroscopic values, quantum calculations may provide microscopic values (i.e. for polyphenols stabilizing Gibbs energies can be evaluated for all OH groups). The relative abundance of each tautomer is therefore evaluated based on trustable (DFT-based) relative Gibbs energies.

3.3. Spectroscopic features

The general case of flavonoids - TD-DFT has repeatedly been used to assess spectroscopic features of flavonoid derivatives. Pure DFT functionals were shown to dramatically underestimate (overestimate) the energies E_{MAX} (wavelength λ_{MAX}) of the maximum absorption band by ca. 0.5 eV (ca. 100 nm at λ = 500 nm).[*,45-46, 54] As expected, adding a HF-like contribution to the exchange term increased E_{MAX}. In the case of flavonoids, the best agreement was obtained with a moderate HF-like percentage (ca. 20-25%), such as with B3LYP and B3P86. The latter functional performed particularly well at predicting λ_{MAX} for a large variety of compounds, including systematic variations of the substituent pattern (mainly OH and OCH_3), as shown by systematic linear regression when plotting calculated against experimental values with a regression coefficient R^2 of 0.9 (Figure 2) but a slight deviation from the ideal regression (slope of 0.88 rather than 1).[45-46] Within the wine pigment family, TD-DFT calculations allowed accurate assignment of λ_{MAX} to the $S_0 \rightarrow S_1$ transition, with a major contribution of the HOMO $\rightarrow$ LUMO electronic excitation (commonly > 70%). The entire spectra of flavonoid derivatives are also well reproduced within this method, i.e., energies and peak intensities (related to oscillator strength) over the entire UV/Vis range.[45]

[*] It is worth noting that spectral shifts should be systematically expressed in terms of energy, as it is the only way to obtain physical meaning. The spectral shift given in terms of wavelength depends on the wavelength at which the measurement was performed, according to $\Delta\lambda = \frac{1}{hc}\lambda^2\Delta E$. Whereas a red-shift of 0.5 eV (ca. 4000 cm^{-1}) corresponds to a 16 nm wavelength shift at 200 nm, the shift is 101 nm at 500 nm.

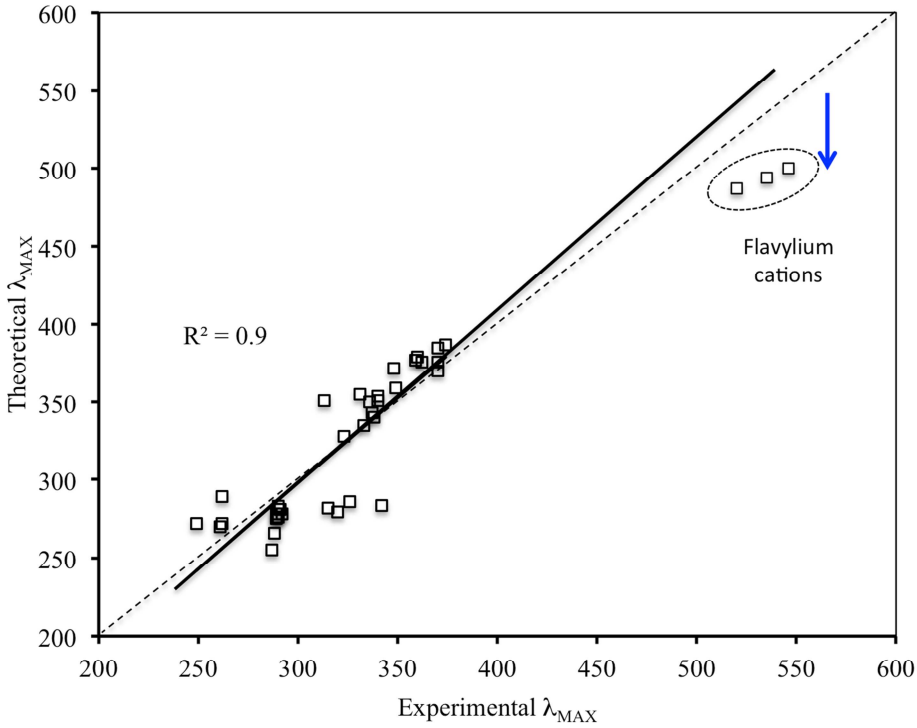

Figure 2: IEFPCM-TD-B3P86/6-31+G(d,p) theoretical maximum absorption wavelength vs. experimental maximum absorption wavelength for a series of ca. forty different flavonoids.

Anthocyanins and the flavylium cation - A significant underestimation of λ_{MAX} (higher than 0.2 eV, i.e., 40 nm at 500 nm) has been systematically observed for anthocyanidin derivatives (flavylium cation form) with hybrid functionals.[45] As a consequence, if the anthocyanidins are removed from the regression calculated in Figure 2, the correlation coefficient (R^2 = 0.8) becomes slightly lower than the overall coefficient (R^2 = 0.9, see Figure 2), but the slope is close to 1 and the intercept to 0. The double-zeta basis set 6-31G(d) once again appears limited, thus larger basis sets are recommended.

An interesting comparison has been made between semi-empirical ZINDO//AM1 and *PCM*-TD-DFT//DFT.[52] Whereas ZINDO provided a rather good description of λ_{MAX} for the flavylium cation, it severely failed at describing the quinonoidal conjugated bases. The latter

might be partly related to the use of AM1 for geometry optimization, which has been shown to cause serious problems with π-conjugated systems (vide supra).

Pyranoanthocyanins - Further ZINDO calculations based on DFT(B3LYP/6-31G(d)) geometries were performed to rationalize the color changes of vinylpyranoanthocyanin-phenolic pigments (Figure 1) upon cooling,[*,55] based on temperature-dependent deviation from planarity[56] that is associated with a loss of π-conjugation and decrease of λ_{MAX}.

More recently, conductor-like *(C)PCM*-TD-PBE0/SV(P) calculations were performed on a series of pyranoanthocyanins.[57] TD-DFT yielded rather good agreement with experimental λ_{MAX} values for all flavylium cations. Stabilizing intramolecular hydrogen bonds, mainly with the sugar moiety, were described, highlighting problems associated with replacing the sugar moiety by a methoxy substituent in the calculations, as these inter- and intramolecular weak interactions may influence not only the conformation but also the optical properties.[†] The CT character of the HOMO → LUMO electronic transition was adequately described. Although, a qualitative understanding of the optical properties could be drawn by TD-DFT, the method failed to quantify in detail the differences between the various pyranoanthocyanins due to rather subtle substituent effects.

To sum up the spectroscopic part, TD-DFT methods using hybrid functionals give a reasonably good description of the optical properties of wine pigments; again, large basis sets tend to improve the results. It should be stressed that standard hybrid functionals only perform well for medium sized π-conjugated systems,[28] a group that wine pigments (accidentally) fall into. For longer π-conjugated systems, offset-corrected TD-DFT has been proposed.[29, 58-60]

[*] In the study, the sugar group at C3 was replaced by a methyl group, an approximation that usually holds as long as no bulky steric interactions or hydrogen bonding are operative.

[†] The reader must be aware that using PCM instead of explicit water molecules, intramolecular hydrogen bonding could be overestimated. This issue is discussed farther in section 6.

4. Copigmentation

Investigation of copigmentation and subsequent spectral modifications with respect to the corresponding free pigments is computationally challenging as the association of (co)pigments is mainly driven by non-covalent interactions, primarily π-stacking, assisted especially by (multiple) OH-substitution and the resulting electron distribution (Figure 3).[11, 13, 21, 47] The few computational works on the description of copigmentation between phenolic derivatives have largely taken advantage of recent developments on description of non-covalent interactions in the field of DFT .[61, 47, 62]

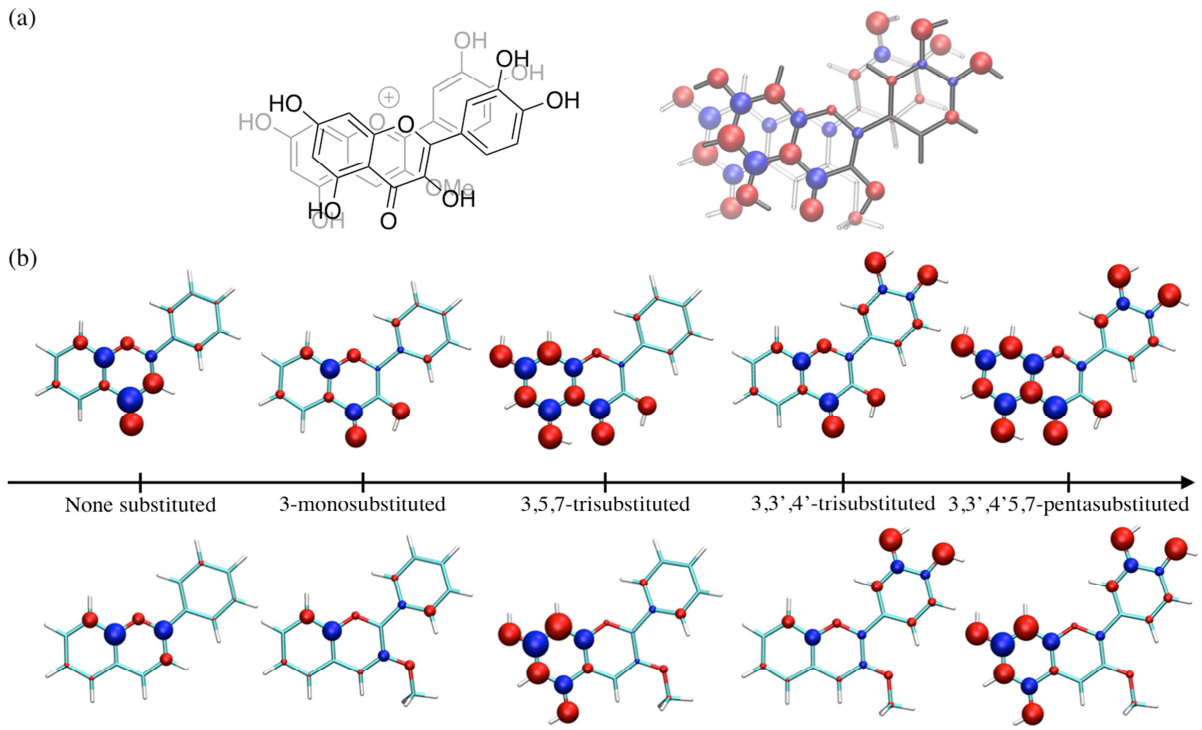

Figure 3. a) Charge distribution in both pigment (3-OMe-cyanindin) and copigment (quercetin), showing adaptability for p-stacking interactions. b) Evolution of charge distribution vs. OH and OCH_3 substitution (number and position; Top: 2-phenylbenzopyrone, Bottom: 2-phenylbenzopyrylium)

4.1. Geometrical issues (from MD to DFT-D), a matter of conformational space sampling

The only experimental way to obtain geometrical information regarding supramolecular arrangements in non-covalent copigmentation complexes in solution is by using NOESY-NMR. Aggregation of flavylium cations with chalcones has been shown to be a multi-aggregation process, confirming the importance of a complete exploration of the conformational space in solution.[63] NOESY-NMR data have provided evidence of theaflavin self-association and theaflavin-caffeine complexation.[64] The π–π and hydrogen bond intermolecular interactions were favored by a spatial arrangement in which the electron deficient tropolone ring lies directly over the electron-rich catechol ring.

From a theoretical point of view, MD simulations have been carried out to investigate association complexes of the oenin pigment (Figure 1) with epicatechin, epigallocatechin, oenin-(O)-C and the procyanidin B3,[65] showing that the complexes were stabilized by dispersive interactions, hydrogen bonding (due to the numerous OH groups in the glucose and phenolic moieties) and hydrophobic effects (release of water molecule from the inter-fragment space). When performed on a sufficient time scale, MD simulations allow random sampling of the conformational space of the copigmentation association process at the classical level of theory. However, if "sufficient" time is not possible, other enhanced sampling techniques (e.g., simulated annealing) must be applied, which should be carried out carefully to avoid over-stabilization in deep local minima. When NMR-NOESY data are available, the use of restrained simulated annealing may be particularly relevant as performed in Ref [64].

Evaluation of the conformational features of copigmentation complexes at the QC level is much more time consuming. Moreover, the inadequate description of dispersive forces that has been observed within the DFT formalism, due to its local nature, was only solved recently. Three main formalisms have been developed and tested over the past decade:[61] *i)* DFT-NL, also commonly named vdW-DF, which intrinsically includes dispersion with a non-

local kernel; *ii)* some of the most highly parameterized methods (e.g., M06-2X), which in some cases exhibit a noisy potential energy surface (as observed for phenolic copigmentation);[47] and *iii)* possibly the most popular, empirically corrected DFT-D theory in a few variants (DFT-D2 and DFT-D3). For systems with a rather limited number of degrees of freedom, a systematic procedure can be used, i.e., scanning the intermolecular distance between the pigment and copigment in the 3D space of (*x*, *y*, *z*) Cartesian coordinates. This procedure allows a detailed analysis of the conformational hypersurface but is usually not suitable for large and non-planar pigments or copigments, such as anthocyanin dimers, polymers, pyranoanthocyanin-flavanols and vinylpyranoanthocyanin-flavanols. We have successfully performed the systematic 3D scanning for the pair formed after aggregation of 3-OMe-cyanidin (pigment in its flavylium form) and quercetin (copigment), within the DFT-D formalism.[47]

4.2. Association energies from MM-PBSA to DFT-D and other refinements

At the classical level (molecular mechanics - MM - calculations), there are various ways to evaluate association energies, the most common being MM-PBSA (molecular mechanics-Poisson Bolzmann/surface area). Association energies between oenin and epicatechin, epigallocatechin, oenin-(O)-C and B3 have been evaluated using the MM-PBSA procedure, which confirmed the hierarchy of the copigment efficiency.[65]

Association energies can also be evaluated at the QC level. When accounting for all possible conformers and calculating energies of association weighted according to Boltzmann distribution, we obtained agreement with the experimental enthalpy of association for the 3-OMe-cyanidin:quercetin complexation.[47, 66] It is worth noting that non-covalent association may also be affected by basis set superposition error (BSSE) arising from basis set incompleteness issues, which artificially overstabilizes the complex formed. Except when

large basis sets are used, this spurious energy can be removed by using a correction known as the counterpoise (CP) method. (see Ref. [47]) CP has been increasingly reported to overestimate BSSE. Therefore, The use of a large basis set (minimum QZVP for DFT calculations and CBS for post-HF methods) remains the best way to avoid BSSE.[67-68]

To obtain a realistic evaluation of association energies, it is mandatory to account for all possible geometries. Therefore, if the pigment-copigment molecular system is too complex for a systemic investigation of the conformational space at the QM level, a combined MD-followed-by-QM approach can be used (see section 6).

4.3. Optical properties and charge transfer excited states

The spectral features of the copigmentation complexes (pigment and copigment, covalently or non-covalently linked) may be significantly changed with respect to the free pigment.[*] In most of cases, copigmentation induces bathochromic shifts. As an example, such bathochromic shifts (by 25 nm, corresponding to red-to-purple hue evolution) observed for two anthocyano-ellagitannin hybrid pigments at wine pH compared to the corresponding anthocyanin and anthocyanidin derivatives could not be rationalized based on ZINDO//AM1 and TD-B3LYP/6-31G(d) calculations.[72] Even though the spectral effect was clearly due to the intramolecular interactions between pigment and copigment, this level of calculations failed at properly describing the complexity of the observed optical behavior, partially attributed to CT in these complexes. With semi-empirical methods or inadequate DFT functionals, the ES description is erroneous when CT plays a significant role. Post-HF methods may circumvent this drawback but have expensive computational costs and do not

[*] The spectroscopic changes induced by the association of two identical chromophores (or structurally similar chromophores, e.g., anthocyanins and flavonols) are usually calculated within the (quantum-chemically modified) Kasha model.[69-70] Here, H- and J-type aggregations enable classification of the observed shifts and relative oscillator strengths of the resulting transitions. If the directional CT character is considerable (strong MO offset between donor and acceptor), the Kasha model ceases to work and the shifts are essentially dependent on the composition and ordering of the resulting frontier MOs.[71]

allow calculation of solvation effects. Based on PBE0/TZVP geometries, the second-order approximate coupled cluster (CC) approach CC2/aug-cc-pVDZ has been successfully applied to evaluate CT in isoflavonoid fluorescence, including microsolvation.[73] Here, daidzein was microsolvated with different numbers of water molecules but always one per OH group. Microsolvation may partially account for explicit intermolecular hydrogen bonding, however even the first solvation shell may include up to six water molecules per OH groups.[74] QM/MM procedures appear more adequate (see section 6.2).

The well known overpolarization issue that makes many DFT exchange-correlation (XC) functionals inadequate for treating CT states can also be overcome within the DFT formalism by using the recently developed RSH functionals, including the correct asymptotic behavior at long distance when charge separation applies, such as CAM-B3LYP or the family of ωB97 methods.[75-77] Based on B3P86-D2(s_6=0.78)/cc-pVDZ geometries, we recently used the ωB97X-D functional to evaluate the spectral shift observed from 3-OMe-cyanidin to the 3-OMe-cyanidin:quercetin copigmentation complex.[47] The bathochromic shift of λ_{MAX} was accurately predicted (ca. 20 nm). This accurate description of the ES allowed an accurate description of the MO diagram. The bathochromic shift was rationalized in terms of a new $S_0 \rightarrow S_1$ transition with strong CT character. This excitation was mainly attributed to the HOMO → LUMO electronic transition, both MOs being borrowed from the copigment (quercetin) and pigment (3-OMe-cyanidin flavylium cation), respectively. Tests against experimental data available for this copigmentation prototype (3-OMe-cyanidin:quercetin complex) validated the SS-PCM-TD-ωB97X-D//cc-pVDZ//*COSMO*-B3P86-D2(s_6=0.78)/cc-pVDZ scheme and opened up prospects for the rationalization and prediction of spectral shifts occurring for wine pigments within the copigmentation process.

Based on this methodology, intramolecular copigmentation effects were also explained for malvidin 3-*O*-glucoside *p*-coumaroyl ester and malvidin 3-*O*-glucoside caffeoyl ester,[78] and

for the copigmentation process between catechin-(4→8)-oenin (the pigment) and three copigments (two epimeric vinylcatechin dimers and one catechin dimer).[79]

5. Molecular orbital analysis

More than just providing spectral values (λ_{MAX} and spectral shifts), QC calculations provide a comprehensive MO description, allowing a deeper understanding of the light absorption process. For wine pigments, the maximum absorption wavelength, assigned to $S_0 \rightarrow S_1$), is mainly described by the HOMO → LUMO electronic transition (ca. 60-70 %) but other $\pi \rightarrow \pi^*$ electronic transitions may contribute to describe the ESs. Moreover, the higher energy bands (assigned to S_2, S_3…) are often complex, requiring configuration interaction with several electronic transition contributions.[45]

In the copigmentation complex between quercetin (donor; D) and 3-O-methylcyanidin (acceptor; A), the resulting HOMO (LUMO) is entirely localized on D (A), see Figure 4, left-hand side.[47] Thus, in a simple one-electron picture, the HOMO → LUMO transition is governed by complete CT. However, in reality, the configuration interaction (CI) description is rather complex. An efficient MO description can be obtained via natural transition orbitals (NTO), i.e., plotting the global MO distributions for GS and ES weighted by the CI coefficients of all MOs involved in the electronic transition (Figure 4, right-hand side). This description provides a much clearer picture of the CT in D-A complexes, showing in the present case that the C2-C3 bond plays a crucial role in rationalizing the copigmentation effect. Thus, NTO MO-CI analysis is recommended in most of cases, especially for ES with complex CI descriptions.

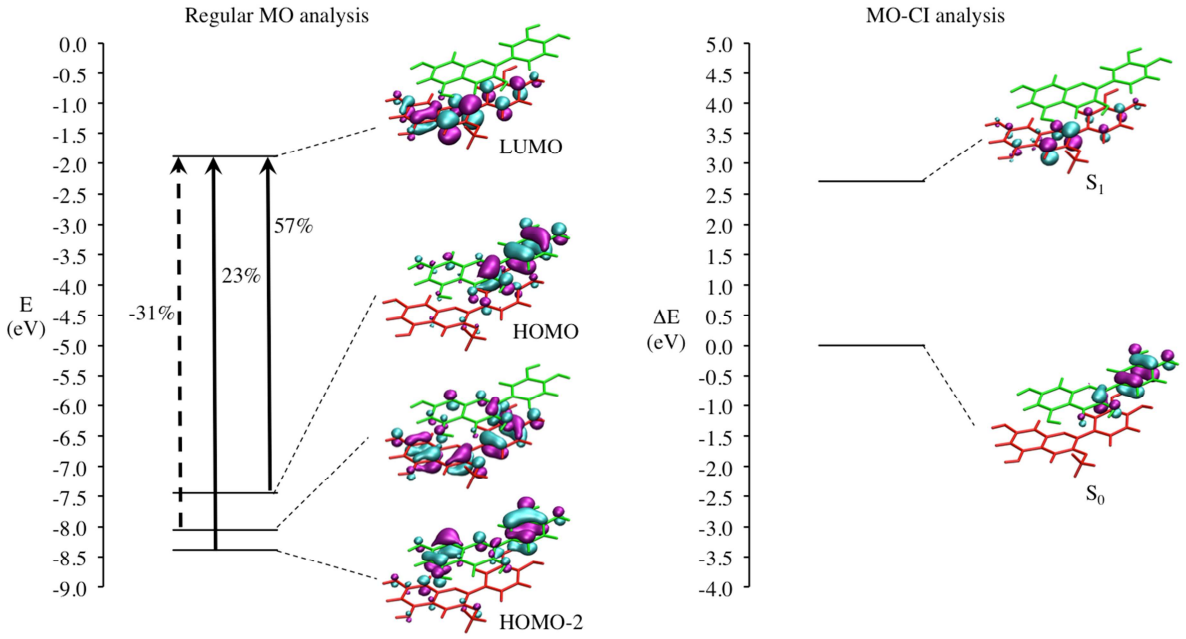

Figure 4: Molecular orbital diagram using a conventional MO representation (left) or a weighted MO-CI analysis (right).

6. Taking environmental conditions into account

Taking solvent effects into account is crucial, particularly when dealing with charged species like the flavylium cations and studying molecular systems in which CT plays a role. Solvent effects also participate in band broadening, which influences the observed spectroscopic features.

6.1. From the gas phase to SS-PCM via conventional PCM

Many different implicit solvent models have been developed based on different formalisms (e.g., multipole expansion (MPE), apparent surface charge (ASC) or generalized Born (GB) methods). The most commonly used are COSMO[80] and PCMs,[81] mainly IEFPCM and (C)PCM (see previous sections). Interestingly, the inclusion of bulk solvation effects, through the (C)PCM model, lowers the absorption maxima and slightly intensifies the transition strengths, giving better agreement with experimental λ_{MAX}.[57]

The combination of continuum models with ES calculation methods has become very challenging over the past years. Due to the success of TD-DFT in allowing a very competitive accuracy/computational ratio, the application of PCM together with TD-DFT has attracted particular attention. The effective Hamiltonian is defined in a static way, whereas the electronic vertical transition is a dynamical problem. Therefore, the conventional application of PCM within TD-DFT calculations ignores the time dependence of solvent relaxation. Different approaches have been developed to overcome this weakness.[81] They may be divided into two families,[82] namely state-specific (SS) and linear-response (LR) methods.

For the 3-OMe-cyanidin:quercetin copigmentation prototype, (*SS-PCM*)-TD-ωB97XD/cc-pVDZ//(*COSMO*)-B3P86-D2(s_6=0.78)/cc-pVDZ predicts a bathochromic shift of 22.9 nm. This is consistent with the bathochromic shift of the cyanidin:quercetin copigmentation complex obtained experimentally (11.7 nm).[66] The use of conventional PCM seemed to give better agreement with experiment. However, the shift was probably slightly underestimated under the experimental conditions as complete complexation is rarely reached.[83] This suggests that the trend obtained with SS-PCM is in better agreement with most experimental observations, confirming the expected improvement.

6.2. Further developments: toward explicit solvent description

Implicit models suffer from a fundamental problem in that they only describe the solvent as an electrostatically interacting system with the solute, thus neglecting specific solute-solvent interactions, such as hydrogen bonding, halogen bonding or π-stacking. In wine chemistry, these interactions may drastically influence the global behavior as the many OH groups of flavonoid derivatives may interact with protic solvents (e.g., water and alcohol) through relatively strong hydrogen bonding interactions. One successful approach is to explicitly describe solvent molecules by a QM/MM approach using a fully self-consistent polarizable

embedding (PE) scheme.[84-85] The idea is to average solvent effects by taking several snapshots along a MD trajectory performed with an explicit solvent and at room temperature so as mimic realistic conditions. The snapshot selection must be as representative as possible of the whole MD simulation.[86] PE-QM/MM calculations are carried out on each snapshot, in which solute molecules are described at the QM level of theory and solvent molecules are described by MM polarizable charges (Figure 5a). UV/Vis absorption properties can easily be calculated from TD-DFT for the QM region, where the GS density is calculated by including self-consistent polarizable solvent effects from the MM region.

Conformational features from MD simulations - The present MD simulations agreed with our previous systematic QM exploration of the 3-OMe-cyanidin:quercetin potential energy surface, yielding five different arrangements close in energy.[47] The $\vec{v}_{QOH}$ and $\vec{v}_{MeCyOH}$ vectors were defined by the C7 and C2 atoms of each partner (quercetin and 3-OMe-cyanidin, respectively). Therefore, $cos(\vec{v}_{QOH}, \vec{v}_{meCyOH})$ represented the orientation of each partner with respect to the other, lying in the range [-1.0 , -0.5] and [0.5 , 1.0] for antiparallel and parallel orientations, respectively. When sampling over a 100 ns simulation, a half and half distribution was obtained for antiparallel and parallel orientations (*D* = 47% for both orientations, see Figure 5b) in agreement with the systematic QM investigation*.

* It must be stressed that the same distribution was observed when 50 snapshots were taken from the 100 ns MD simulations, confirming that the averaging for the rationalization of UV/Vis absorption properties is sufficient.

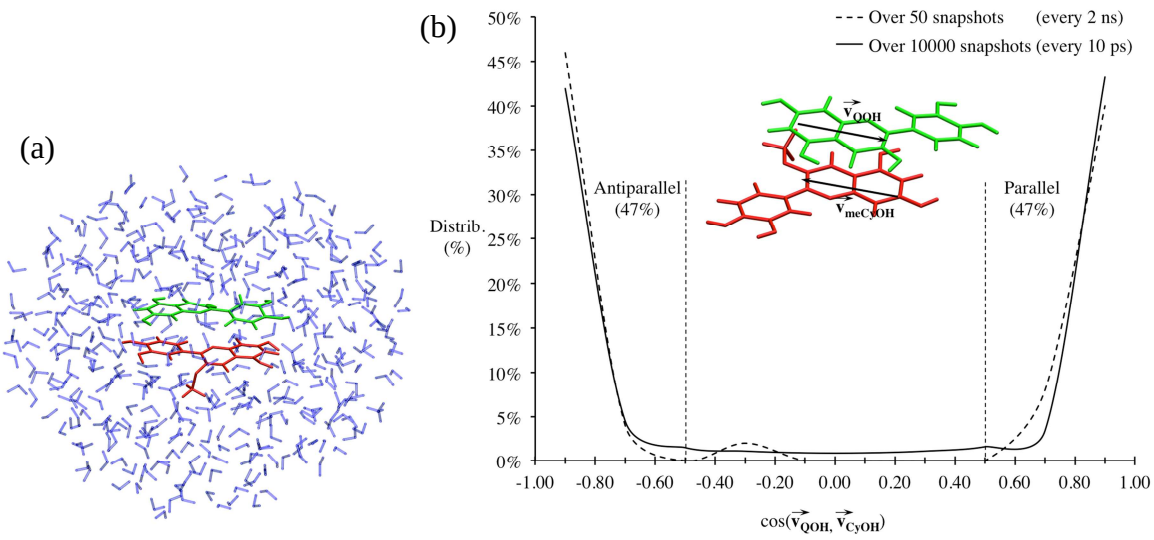

Figure 5: a) PE-QM/MM derived snapshot for the 3-OMe-cyanidin:quercetin copigmentation complex. Quercetin, 3-O-methylcyanidin and water molecules are in green, red and blue, respectively. b) Distribution of $cos(\vec{v}_{QOH}, \vec{v}_{meCyOH})$ over 100ns MD simulation (bold line) and selection of 50 snapshots (dashed line).

In water, phenolic wine pigments and copigments are expected to strongly interact with the solvent through intermolecular hydrogen bonding due to the high number of OH groups. Therefore, intermolecular solute-solvent hydrogen bonding appears strong enough to decrease the occurrence of the intramolecular hydrogen bonds, like in quercetin. Namely, the 3-OH---O4, 3'-OH---O4' and 4'-OH---O3' hydrogen bonds exhibited low distributions (28.9 %, 1.5% and 10.9%, respectively, see Table 1). The 5-OH---O4 intramolecular hydrogen bond of quercetin is strong enough to occur 98.6% of the MD simulation time. No significant intermolecular hydrogen bonding was observed between the two partners of the quercetin:3-OMe-cyanidin copigmentation complex, again in agreement with the previous QM evaluation.[47] In other words, the MD simulation confirms our previous findings that quercetin:3-OMe-cyanidin copigmentation is mainly driven by dispersive interactions.[47]

Predicting the copigmentation bathochromic shift with explicit solvation - As already seen with pure TD-DFT calculations, the (*PE-QM/MM*)-TD-CAM-B3LYP/aug-cc-pVDZ vertical excitation energy of the flavylium cation was blue-shifted by 0.36 eV with respect to the experimental value (cf. a shift of 0.41 eV with (*SS-PCM*)-TD-ωB97XD/cc-pVDZ [47]). The PE-QM/MM method predicted a bathochromic shift (13.0 nm) lying in the range of experimental values.[66, 83] It appeared closer than the spectral shift obtained by the former reference (11.7 nm) and lower than the full QM ((*SS-PCM*)-TD-ωB97XD/cc-pVDZ) prediction. This method is particularly promising as it provides an explicit solvation description, accounting for the role of solute-solvent intermolecular interactions. For the 3-OMe-cyanidin:quercetin copigmentation system, 100 ns MD simulations allowed correct sampling of the conformational space. This method mimics a realistic environment by accounting for all inter- and intra-molecular driving forces of the copigmentation process. All geometrical descriptors can thus be averaged over the simulation time scale, providing a description as close as possible to the experimental observations. In particular, the method intrinsically predicts line broadening due to solvent.[*]

7. Conclusion: guidelines

The molecular and electronic description of wine pigments has benefitted from recent and constantly evolving molecular modeling methods, in particular within the DFT framework. However, non-specialists might easily get lost in the forest of different functionals and their specific applicability. We would therefore like to finish the current overview by providing some practical and accurate guidelines on how to use molecular modeling for non-specialists, e.g., in food academic labs and industries.

[*] The vibrational broadening should be recalculated by appropriate methodologies.

1- The geometrical features of wine pigments can be well predicted with DFT hybrid functionals (e.g., B3P86, B3LYP, PBE0). Double-zeta basis sets with a polarization function on heavy atoms are the minimum requirement (e.g., 6-31G(d), cc-pVDZ and SVP for Pople's, Dunning's and Ahlrichs' type basis sets, respectively). However, it is recommended that a triple-zeta basis set is used and diffuse functions added to account for possible charged species, as well as polarization functions on hydrogens (e.g., 6-311+G(d,p), aug-ccpVTZ and Def2-TZVPP for Pople's, Dunning's and Ahlrichs' type basis sets, respectively).[*]

2- The optical properties of molecules in solution (maximum absorption wavelength λ_{MAX}, oscillator strength *f*, substitution effects) can also be assessed with hybrid functionals. The qualitative description is accurate with all hybrid functionals or further functional generations, allowing the establishment of relevant structure-property relationships. With almost all functionals, λ_{MAX} is underestimated for the flavylium cation, but PBE0 and B3P86 are the best performing. According to the functional used, an offset can be parameterized and safely used for related derivatives. Regarding basis sets, similar recommendations are proposed as for the geometrical features.

3- The conformational prediction of copigmentation complexes must be achieved by using DFT functionals that include dispersive terms (within the DFT-D and DFT-NL formalisms). Non-corrected functionals fail at finding stable copigmentation complexes. When the copigmentation systems exhibit too many degrees of freedom, a preliminary MD simulation is mandatory. However, this must be carefully performed to ensure sufficiently robust sampling of the conformational space, e.g., by using simulated annealing procedures, to obtain all possible supramolecular arrangements.

[*] Depending on the software used, working habits and speedup algorithms, one can use the Pople, Dunning or Ahlrichs type basis sets; other types of basis sets are available in different codes, but the three mentioned are the most widely used.

4- To accurately assess the optical properties, i.e., spectral shifts in copigmentation complex with respect to the isolated pigments, CT must be comprehensively and accurately described, which can be obtained at a reasonable computational time with RSH functionals, such as CAM-B3LYP or ωB97X-D. This is a critical issue, as the use of non-adequate functionals would fail to describe CT, therefore completely missing the copigmentation effect (e.g., bathochromic shifts).

5- The use of solvent models (at least implicit) is mandatory, especially as most wine pigments are charged, being in their flavylium cation form. Even when dealing with neutral forms, equilibrium constants with the charged forms should be predicted and accuracy is only reached by using at least a PCM solvent. (C)PCM has been shown to enhance the λ_{MAX} prediction of flavylium cations. CT description also requires the inclusion of solvent effects. The use of TD-DFT has more physical meaning if it is combined with SS-PCM of LR-PCM; these methods are recommended but still require careful benchmarking.

6- All further developments should be carefully considered. In particular, new QM/MM developments allow a complete description of intermolecular interaction with protic solvents, which may play a crucial role in wine pigmentation.

8. Computational details

MD Simulations - Force field parameters for quercetin and 3-OMe-cyanidin (Figure 1) were derived from B3P86/6-31+G(d,p) calculations. Partial atomic charges were assigned using the Antechamber and RESP programs after single point calculations with HF/6-31G* using Gaussian09.[87]

Two MD simulations were performed for either stand-alone 3-OMe-cyanidin or quercetin:3-OMe-cyanidin copigmentation complexes in water, with one chloride counterion in both cases to reach a neutral system and avoid Ewald summation issues during the

dynamics. The generalized atom force field (GAFF) as implemented in the Amber package[88] was used to perform 100 ns MD simulations with an integration step of 2 fs. All MD simulations were carried out in a canonical ensemble at 300 K using Langevin's thermostat with collision frequency of 1 ps^{-1}. MD simulations were performed within the SHAKE algorithm constraining all bonds involving hydrogen. Water molecules were described by the "three-point" TIP3P model. The simulations were carried out in a thermally equilibrated water box of 39.8x34.8x39.0 $Å^3$ and 40.5x37.3x38.8 $Å^3$ for 3-OMe-cyanidin and quercetin:3-OMe-cyanidin, respectively, corresponding to a water density of 1.0 $g.cm^{-3}$. Fifty independent snapshots (taken every 2 ns) were used for the UV/Vis QM calculations.

PE-QM/MM calculations of UV/Vis properties - TD-DFT calculations were carried out with the Coulomb attenuated B3LYP (CAM-B3LYP) functional known to accurately predict ES-CT. The aug-cc-pVDZ basis set was used in all calculations for the QM region. The MM region included all water molecules within a radius of 1 nm, which has been shown to be sufficient for describing solvent effects.[86] The MM Ahlström's potential (including atomic charges and polarizabilities)[89] was used for all water molecules, whereas chloride counterions were defined as non-polarizable -1 point charges. All PE-QM/MM calculations were carried out using the DALTON package.[90]

Acronyms

AM1 Austin Model 1; **ASC** Apparent Surface Charge; **BSSE** Basis Set Superposition Error; **CAM-B3LYP** Coulomb-Attenuated Method B3LYP; **CC** Coupled-Cluster; **CC2** Second order approximate Coupled Cluster; **CI** Configuration Interaction; **COSMO** COnductor-like Solvation MOdel; **CP** Counterpoise; **CPCM** Conductor-like Polarizable Continuum Model; **CT** Charge Transfer; **CT-ES** Charge Transfer in Excited State; **DFT** Density Functional Theory; **DFT-D** Dispersion-corrected Density Functional Theory; **DFT-NL** Non-Local Density Functional Theory; **ES** Excited State; **GAFF** Generalized Amber Force Field; **GB** Generalized Born; **GS** Ground State; **HF** Hartree-Fock; **HMO** Hückel Molecular Orbital; **HOMO** Highest Occupied Molecular Orbital; **IEFPCM** Integral Equation Formalism Polarizable Continuum Model; **INDO** Intermediate Neglect of

Differential Overlap; **LR** Linear Response; **LUMO** Lowest Unoccupied Molecular Orbital; **MD** Molecular Dynamics; **MM** Molecular Mechanics; **MM-PBSA** Molecular Mechanics- Poisson Bolzmann/Surface Area; **MO** Molecular Orbital; **MPE** MultiPole Expansion; **NMR** Nuclear Magnetic Resonance; **NOE** Nuclear Overhauser Effect; **NOESY** Nuclear Overhauser Effect SpectroscopY; **NTO** Natural Transition Orbital; **PCM** Polarizable Continuum Model; **PE** Polarizable Embedding; **PPP** Pariser-Parr-Pople; **QC** Quantum Chemistry; **QM** Quantum Mechanics; **QSPR** Quantitative Structure Property Relationship; **RESP** Restricted ElectroStatic Potential; **RI** Resolution of the Identity; **RSH** Range-separated Hybrid; **SCS** Spin-Component-Scaled; **SS-PCM** State-Specific Polarizable Continuum Model; **TD** Time-Dependant; **TD-DFT** Time-Dependant Density Functional Theory; **UV** Ultraviolet; **UV/Vis** Ultraviolet/Visible; **vDW-DF** van der Waals Density Functional; **ZINDO** Zerner's Intermediate Neglect of Differential Overlap

Acknowledgements

PT thanks INSERM and the “Conseil Régional du Limousin”. Financial support from the Czech Science Foundation (P208/12/G016), the Operational Program Research and Development for Innovations-European Regional Development Fund (project CZ.1.05/2.1.00/03.0058 of the Ministry of Education, Youth and Sports of the Czech Republic), the Barrande project (No. 7AMB12FR026) and the Operational Program Education for Competitiveness-European Social Fund (project CZ.1.07/2.3.00/20.0017 of the Ministry of Education, Youth and Sports of the Czech Republic) are also gratefully acknowledged. The work at IMDEA was supported by the Spanish Ministerio de Economía y Competitividad (MINECO; project CTQ2011-27317). ML thanks the Swedish e-Science Research Center (SeRC) for financial support. FDM and ML thank the Swedish National Infrastructure for Computing (SNIC) for providing resources at the National Supercomputer Centre (NSC), Sweden. The authors thank G. Fabre and Prof. P. Norman for fruitful scientific discussions.

References

(1) Cheynier, V.; Dueñas-Paton, M.; Salas, E.; Maury, C.; Souquet, J.-M.; Sarni-Manchado, P.; Fulcrand, H. *Am. J. Enol. Vitic.* **2006,** *57*, 298-305.

(2) Freitas, V.; Mateus, N. *Anal. Bioanal. Chem.* **2011,** *401*, 1463-1473.

(3) Fulcrand, H.; Dueñas, M.; Salas, E.; Cheynier, V. *Am. J. Enol. Vitic.* **2006,** *57*, 289-297.

(4) Pina, F.; Melo, M. J.; Laia, C. A. T.; Parola, A. J.; Lima, J. C. *Chem. Soc. Rev.* **2012,** *41*, 869-908.

(5) Mateus, N.; Carvalho, E.; Carvalho, A. R. F.; Melo, A.; González-Paramás, A. M.; Santos-Buelga, C.; Silva, A. M. S.; de Freitas, V. *J. Agric. Food Chem.* **2002,** *51*, 277-282.

(6) Mateus, N.; Oliveira, J.; Haettich-Motta, M.; de Freitas, V. *J. Biomed. Biotechnol.* **2004,** *2004*, 299-305.

(7) Mateus, N.; Oliveira, J.; Pissarra, J.; González-Paramás, A. M.; Rivas-Gonzalo, J. C.; Santos-Buelga, C.; Silva, A. M. S.; de Freitas, V. *Food Chem.* **2006,** *97*, 689-695.

(8) He, J.; Oliveira, J.; Silva, A. M. S.; Mateus, N.; De Freitas, V. *J. Agric. Food Chem.* **2010,** *58*, 8814-8819.

(9) Chassaing, S.; Isorez, G.; Kueny-Stotz, M.; Brouillard, R. *Tetrahedron Lett.* **2008,** *49*, 6999-7004.

(10) Oliveira, J.; Mateus, N.; Freitas, V. d. *Tetrahedron Lett.* **2011,** *52*, 1996-2000.

(11) Brouillard, R.; Mazza, G.; Saad, Z.; Albrecht-Gary, A. M.; Cheminat, A. *J. Am. Chem. Soc.* **1989,** *111*, 2604-2610.

(12) Goto, T.; Kondo, T. *Angew. Chem. Int. Ed.* **1991,** *30*, 17-33.

(13) Dangles, O.; Brouillard, R. *Can. J. Chem.* **1992,** *70*, 2174-2189.

(14) Dangles, O.; Brouillard, R. *J. Chem. Soc., Perkin Trans. 2* **1992**, 10.1039/P29920000247, 247-257.

(15) Malaj, N.; De Simone, B. C.; Quartarolo, A. D.; Russo, N. *Food Chem.* **2013,** *141*, 3614-3620.

(16) Quijada-Morín, N.; Dangles, O.; Rivas-Gonzalo, J. n. C.; Escribano-Bailón, M. T. *J. Agric. Food Chem.* **2010,** *58*, 9744-9752.

(17) Rustioni, L.; Basilico, R.; Fiori, S.; Leoni, A.; Maghradze, D.; Failla, O. *Phytochem. Anal.* **2013,** *24*, 453-459.

(18) Mizuno, H.; Hirano, K.; Okamoto, G. *Vitis* **2006,** *4*, 173-177.

(19) Boyd, G. V.; Singer, N. *Tetrahedron* **1965,** *21*, 1263-1276.

(20) Singer, N.; Whittington, P. R.; Boyd, G. V. *Tetrahedron* **1970,** *26*, 3731-3748.

(21) Velu, S. S.; Di Meo, F.; Trouillas, P.; Sancho-Garcia, J.-C.; Weber, J.-F. F. *J. Nat. Prod.* **2013,** *76*, 538-546.

(22) Leopoldini, M.; Rondinelli, F.; Russo, N.; Toscano, M. *J. Agric. Food Chem.* **2010,** *58*, 8862-8871.

(23) Ueno, K.; Saito, N. *Acta Crystallogr. Sect. B* **1977,** *33*, 114-116.

(24) Rastelli, G.; Costantino, L.; Albasini, A. *J. Mol. Struct. THEOCHEM* **1993,** *279*, 157-166.

(25) Pereira, G. K.; Donate, P. M.; Galembeck, S. E. *J. Mol. Struct. THEOCHEM* **1996,** *363*, 87-96.

(26) Pereira, G. K.; Donate, P. M.; Galembeck, S. E. *J. Mol. Struct. THEOCHEM* **1997,** *392*, 169-179.

(27) Zerner, M. C., Semiempirical Molecular Orbital Methods. In *Reviews in Computational Chemistry*, John Wiley & Sons, Inc.: 2007; Vol. 2, pp 313-365.

(28) Gierschner, J.; Cornil, J.; Egelhaaf, H. J. *Adv. Mater.* **2007,** *19*, 173-191.

(29) Wykes, M.; Milián Medina, B.; Gierschner, J. *Front. Chem.* **2013,** *1*.

(30) Trouillas, P.; Fagnere, C.; Lazzaroni, R.; Calliste, C.; Marfak, A.; Duroux, J.-L. *Food Chem.* **2004,** *88*, 571-582.

(31) Trouillas, P., Marsal, P., Siri, D., Lazzaroni, R., Duroux, J. L. *Food Chem.* **2006,** *97*, 10.

(32) Kozlowski, D.; Trouillas, P.; Calliste, C.; Marsal, P.; Lazzaroni, R.; Duroux, J.-L. *J. Phys. Chem. A* **2007,** *111*, 1138-1145.

(33) Anouar, E.; Calliste, C. A.; Kosinova, P.; Di Meo, F.; Duroux, J. L.; Champavier, Y.; Marakchi, K.; Trouillas, P. *J. Phys. Chem. A* **2009,** *113*, 13881-13891.

(34) Di Meo, F.; Lemaur, V.; Cornil, J.; Lazzaroni, R.; Duroux, J.-L.; Olivier, Y.; Trouillas, P. *J. Phys. Chem. A* **2013,** *117*, 2082-2092.

(35) Leopoldini, M.; Pitarch, I. P.; Russo, N.; Toscano, M. *J. Phys. Chem. A* **2004,** *108*, 92-96.

(36) Leopoldini, M.; Marino, T.; Russo, N.; Toscano, M. *J. Phys. Chem. A* **2004,** *108*, 4916-4922.

(37) Chiodo, S. G.; Leopoldini, M.; Russo, N.; Toscano, M. *Phys. Chem. Chem. Phys.* **2010,** *12*, 7662-7670.

(38) Fiorucci, S.; Golebiowski, J.; Cabrol-Bass, D.; Antonczak, S. *ChemPhysChem* **2004,** *5*, 1726-1733.

(39) Fiorucci, S.; Golebiowski, J.; Cabrol-Bass, D.; Antonczak, S. *J. Agric. Food Chem.* **2007,** *55*, 903-911.

(40) Say-Liang-Fat, S.; Cornard, J. P.; Moncomble, A. *Polyhedron* **2012,** *48*, 237-244.

(41) Cornard, J. P.; Lapouge, C.; André, E. *Spectrochim. Acta A* **2013,** *108*, 280-287.

(42) Le Person, A.; Moncomble, A.; Cornard, J. P. *J. Phys. Chem. A* **2014,** *118*, 2646-2655.

(43) Furia, E.; Marino, T.; Russo, N. *Dalton Trans.* **2014,** *43*, 7269-7274.

(44) Kosinova, P.; Gazak, R.; Duroux, J.-L.; Lazzaroni, R.; Kren, V.; Assfeld, X.; Trouillas, P. *ChemPhysChem* **2011,** *12*, 1135-1142.

(45) Anouar, E. H.; Gierschner, J.; Duroux, J.-L.; Trouillas, P. *Food Chem.* **2012,** *131*, 79-89.

(46) Millot, M.; Di Meo, F.; Tomasi, S.; Boustie, J.; Trouillas, P. *J. Photochem. Photobiol. B* **2012,** *111*, 17-26.

(47) Di Meo, F.; Sancho Garcia, J. C.; Dangles, O.; Trouillas, P. *J. Chem. Theory Comp.* **2012,** *8*, 2034-2043.

(48) Meyer, M. *Int. J. Quant. Chem.* **2000,** *76*, 724-732.

(49) Karpfen, A.; Choi, C. H.; Kertesz, M. *J. Phys. Chem. A* **1997,** *101*, 7426-7433.

(50) Carvalho, A. R. F.; Oliveira, J.; de Freitas, V.; Mateus, N.; Melo, A. *Int. J. Quant. Chem.* **2011,** *111*, 1355-1360.

(51) Carvalho, A. R. F.; Oliveira, J.; de Freitas, V.; Silva, A.; Mateus, N.; Melo, A. *J. Mol. Struct. THEOCHEM* **2010,** *946*, 113-118.

(52) Freitas, A. A.; Shimizu, K.; Dias, L. G.; Quina, F. H. *J. Brazil. Chem. Soc.* **2007,** *18*, 1537-1546.

(53) Peruzzo, P. J.; Marino, D. J. G.; Castro, E. A.; Toropov, A. A. *J. Mol. Struct. THEOCHEM* **2001,** *572*, 53-60.

(54) Di Meo, F.; Trouillas, P.; Adamo, C.; Sancho-García, J. C. *J. Chem. Phys.* **2013,** *139*, -.

(55) Carvalho, A. R. F.; Oliveira, J.; De Freitas, V.; Mateus, N.; Melo, A. *J. Agric. Food Chem.* **2010,** *58*, 4292-4297.

(56) Gierschner, J.; Mack, H.-G.; Lüer, L.; Oelkrug, D. *J. Chem. Phys.* **2002,** *116*, 8596-8609.

(57) Quartarolo, A. D.; Russo, N. *J. Chem. Theory Comp.* **2011,** *7*, 1073-1081.

(58) Champagne, B.; Perpète, E. A.; Jacquemin, D.; van Gisbergen, S. J. A.; Baerends, E.-J.; Soubra-Ghaoui, C.; Robins, K. A.; Kirtman, B. *J. Phys. Chem. A* **2000,** *104*, 4755-4763.

(59) Perpète, E. A.; Wathelet, V.; Preat, J.; Lambert, C.; Jacquemin, D. *J. Chem. Theory Comp.* **2006,** *2*, 434-440.

(60) Preat, J.; Jacquemin, D.; Wathelet, V.; André, J.-M.; Perpète, E. A. *J. Phys. Chem. A* **2006,** *110*, 8144-8150.

(61) Grimme, S. *WIRES: Comp. Mol. Sci.* **2011,** *1*, 211-228.

(62) Bayach, I.; Sancho-García, J. C.; Di Meo, F.; Weber, J. F. F.; Trouillas, P. *Chem. Phys. Lett.* **2013,** *578*, 120-125.

(63) Houbiers, C.; Lima, J. C.; Maçanita, A. L.; Santos, H. *J. Phys. Chem. B* **1998,** *102*, 3578-3585.

(64) Charlton, A. J.; Davis, A. L.; Jones, D. P.; Lewis, J. R.; Davies, A. P.; Haslam, E.; Williamson, M. P. *J. Chem. Soc., Perkin Trans. 2* **2000**, 10.1039/A906380C, 317-322.

(65) Teixeira, N.; Cruz, L.; Brás, N. F.; Mateus, N.; Ramos, M. J.; de Freitas, V. *J. Agric. Food Chem.* **2013,** *61*, 6942-6948.

(66) Dimitric, M. J. M.; Baranac, J. M.; Brdaric, T. P. *Spectrochim. Acta A* **2005,** *62A*, 673-680.

(67) Risthaus, T.; Grimme, S. *J. Chem. Theory Comp.* **2013,** *9*, 1580-1591.

(68) Goerigk, L. *J. Chem. Theory Comp.* **2014,** *10*, 968-980.

(69) Kasha, M.; Rawls, H. R.; Ashraf El-Bayoumi, M. *Pure Appl. Chem.* **1965,** *11*, 371-392.

(70) Gierschner, J.; Park, S. Y. *J. Mater. Chem. C* **2013,** *1*, 5818-5832.

(71) Park, S. K.; Varghese, S.; Kim, J. H.; Yoon, S.-J.; Kwon, O. K.; An, B.-K.; Gierschner, J.; Park, S. Y. *J. Am. Chem. Soc.* **2013,** *135*, 4757-4764.

(72) Chassaing, S.; Lefeuvre, D.; Jacquet, R.; Jourdes, M.; Ducasse, L.; Galland, S.; Grelard, A.; Saucier, C.; Teissedre, P.-L.; Dangles, O.; Quideau, S. *Eur. J. Org. Chem.* **2010,** *2010*, 55-63.

(73) Beyhan, S. M.; Götz, A. W.; Ariese, F.; Visscher, L.; Gooijer, C. *J. Phys. Chem. A* **2011,** *115*, 1493-1499.

(74) Lucarini, M.; Pedulli, G. F.; Guerra, M. *Chemistry – A European Journal* **2004,** *10*, 933-939.

(75) Yanai, T.; Tew, D. P.; Handy, N. C. *Chem. Phys. Lett.* **2004,** *393*, 51-57.

(76) Chai, J.-D.; Head-Gordon, M. *J. Chem. Phys.* **2008,** *128*, 084106.

(77) Chai, J.-D.; Head-Gordon, M. *Phys. Chem. Chem. Phys.* **2008,** *10*, 6615-6620.

(78) Rustioni, L.; Di Meo, F.; Guillaume, M.; Failla, O.; Trouillas, P. *Food Chem.* **2013,** *141*, 4349-4357.

(79) Nave, F.; Brás, N. F.; Cruz, L.; Teixeira, N.; Mateus, N.; Ramos, M. J.; Di Meo, F.; Trouillas, P.; Dangles, O.; De Freitas, V. *J. Phys. Chem. B* **2012,** *116*, 14089-14099.

(80) Sinnecker, S.; Rajendran, A.; Klamt, A.; Diedenhofen, M.; Neese, F. *J. Phys. Chem. A* **2006,** *110*, 2235-2245.

(81) Tomasi, J.; Mennucci, B.; Cammi, R. *Chem. Rev.* **2005,** *105*, 2999-3093.

(82) Improta, R.; Barone, V.; Scalmani, G.; Frisch, M. J. *J. Chem. Phys.* **2006,** *125*, 054103.

(83) Alluis, B.; Dangles, O. *Helv. Chim. Acta* **2001,** *84*, 1133-1156.

(84) Pedersen, M. N.; Hedegård, E. D.; Olsen, J. M. H.; Kauczor, J.; Norman, P.; Kongsted, J. *J. Chem. Theory Comp.* **2014,** *10*, 1164-1171.

(85) Olsen, J. g. M.; Aidas, K. s.; Kongsted, J. *J. Chem. Theory Comp.* **2010,** *6*, 3721-3734.

(86) Sjöqvist, J.; Linares, M.; Mikkelsen, K. V.; Norman, P. *J. Phys. Chem. A* **2014,** *118*, 3419-3428.

(87) Gaussian 09, R. A., Frisch, M. J.; Trucks, G. W.; Schlegel, H. B.; Scuseria, G. E.; Robb, M. A.; Cheeseman, J. R.; Scalmani, G.; Barone, V.; Mennucci, B.; Petersson, G. A.; Nakatsuji, H.; Caricato, M.; Li, X.; Hratchian, H. P.; Izmaylov, A. F.; Bloino, J.; Zheng, G.; Sonnenberg, J. L.; Hada, M.; Ehara, M.; Toyota, K.; Fukuda, R.; Hasegawa, J.; Ishida, M.; Nakajima, T.; Honda, Y.; Kitao, O.; Nakai, H.; Vreven, T.; Montgomery, Jr., J. A.; Peralta, J. E.; Ogliaro, F.; Bearpark, M.; Heyd, J. J.; Brothers, E.; Kudin, K. N.; Staroverov, V. N.; Kobayashi, R.; Normand, J.; Raghavachari, K.; Rendell, A.; Burant, J. C.; Iyengar, S. S.; Tomasi, J.; Cossi, M.; Rega, N.; Millam, N. J.; Klene, M.; Knox, J. E.; Cross, J. B.; Bakken, V.; Adamo, C.; Jaramillo, J.; Gomperts, R.; Stratmann, R. E.; Yazyev, O.; Austin, A. J.; Cammi, R.; Pomelli, C.; Ochterski, J. W.; Martin, R. L.; Morokuma, K.; Zakrzewski, V. G.; Voth, G. A.; Salvador, P.; Dannenberg, J. J.; Dapprich, S.; Daniels, A. D.; Farkas, Ö.; Foresman, J. B.; Ortiz, J. V.; Cioslowski, J.; Fox, D. J. Gaussian, Inc., Wallingford CT, 2009.

(88) Salomon-Ferrer, R.; Case, D. A.; Walker, R. C. *WIRES: Comp. Mol. Sci.* **2013,** *3*, 198-210.

(89) Ahlström, P.; Wallqvist, A.; Engström, S.; Jönsson, B. *Mol. Phys.* **1989,** *68*, 563-581.

(90) Aidas, K.; Angeli, C.; Bak, K. L.; Bakken, V.; Bast, R.; Boman, L.; Christiansen, O.; Cimiraglia, R.; Coriani, S.; Dahle, P.; Dalskov, E. K.; Ekström, U.; Enevoldsen, T.; Eriksen, J. J.; Ettenhuber, P.; Fernández, B.; Ferrighi, L.; Fliegl, H.; Frediani, L.; Hald, K.; Halkier, A.; Hättig, C.; Heiberg, H.; Helgaker, T.; Hennum, A. C.; Hettema, H.; Hjertenæs, E.; Høst, S.; Høyvik, I.-M.; Iozzi, M. F.; Jansík, B.; Jensen, H. J. A.; Jonsson, D.; Jørgensen, P.; Kauczor, J.; Kirpekar, S.; Kjærgaard, T.; Klopper, W.; Knecht, S.; Kobayashi, R.; Koch, H.; Kongsted, J.; Krapp, A.; Kristensen, K.; Ligabue, A.; Lutnæs, O. B.; Melo, J. I.; Mikkelsen, K. V.; Myhre, R. H.; Neiss, C.; Nielsen, C. B.; Norman, P.; Olsen, J.; Olsen, J. M. H.; Osted, A.; Packer, M. J.; Pawlowski, F.; Pedersen, T. B.; Provasi, P. F.; Reine, S.; Rinkevicius, Z.; Ruden, T. A.; Ruud, K.; Rybkin, V. V.; Sałek, P.; Samson, C. C. M.; de Merás, A. S.; Saue, T.; Sauer, S. P. A.; Schimmelpfennig, B.; Sneskov, K.; Steindal, A. H.; Sylvester-Hvid, K. O.; Taylor, P. R.; Teale, A. M.; Tellgren, E. I.; Tew, D. P.; Thorvaldsen, A. J.; Thøgersen, L.; Vahtras, O.; Watson, M. A.; Wilson, D. J. D.; Ziolkowski, M.; Ågren, H. *WIRES: Comp. Mol. Sci.* **2014,** *4*, 269-284.

Supplementary Information

Optical properties of wine pigments: theoretical guidelines with new methodological perspectives

Patrick Trouillas,[a,b,1] Florent Di Meo,[c] Johannes Gierschner,[d] Mathieu Linares,[c] Juan Carlos Sancho-García,[e] and Michal Otyepka[b]

[a]INSERM S850, Université de Limoges, 2 rue du Dr Marcland, F-87025 Limoges, France

[b]Regional Centre of Advanced Technologies and Materials, Department of Physical Chemistry, Faculty of Science, Palacký University of Olomouc, tr. 17. listopadu 12, 771 46 Olomouc, Czech Republic

[c]Department of Physics, Chemistry and Biology (IFM), Linköping University, SE-58183 Linköping, Sweden

[d]Madrid Institute for Advanced Studies - IMDEA Nanoscience, C/ Faraday 9, Ciudad Universitaria de Cantoblanco, E-28049 Madrid, Spain

[e]Departamento de Química Física, Universidad de Alicante, Apartado de Correos 99, E-03080 Alicante, Spain

[1] Corresponding author. Tel. : +33 555 435 927, e-mail address: patrick.trouillas@unilim.fr

Brief introduction to molecular modeling methods

Since this article is primarily written for users (chemists and physicists of natural compounds and oenologists working on genotyping and phenotyping) rather than specialists in theoretical chemistry, we first present some basic concepts and discuss the variety of methods available, each with their own pros and cons, which thus form the core of current computational chemistry.

At the lowest end of this hierarchy is molecular mechanics (MM), which is based on classical physics and mainly designed to provide structural information. MM uses an empirical force field (FF) for the energy expression, covering covalent and non-covalent interactions at a very approximate level, MM does not explicitly consider electrons. Despite their limitations, FFs can be used to at least preliminary predict conformational features of (supra)molecular arrangements in wine chemistry. Introducing temperature (atom velocities), i.e., performing molecular dynamics (MD), allows relevant descriptions of molecular assemblies.

When dealing with thermodynamic, kinetics and optical properties of wine pigments in a nanoscopic size regime where quantum effects truly manifest, one must consider quantum mechanics (QM) methods, i.e., seeking to solve the underlying Schrödinger equation. These methods are known as wavefunction approaches. The basic approach toward solving the Schrödinger equation is the Hartree-Fock (HF) method, which (by definition) neglects electron correlation effects, and hence provides a rather poor description of many properties of π-conjugated systems (e.g., it fails to describe non-covalent π-π interactions). Semi-empirical methods e.g., AM1 (Austin model 1), PM3 (parameterized model 3) and INDO/S (intermediate neglect of differential overlap / for spectroscopic applications) are even more approximate than the HF method (neglecting and/or approximating some bi-electronic interactions). However, they may provide a reasonable qualitative description of π-conjugated systems thanks to adequate parameterizations over well-chosen training sets. Nevertheless, most of these

methods underestimate the strength of π-conjugation, leading to several drawbacks, mainly affecting the accurate evaluation of optical properties in the UV/Vis range, which need to be identified and (possibly) eliminated in order to improve performance. Note that the main advantage of the latter methods is their low computational cost compared to other approaches. Post-HF (i.e., perturbative or projective) methods (e.g., Møller-Plesset (MP)2, spin-component scaled (SCS)-MP2, coupled-cluster (CC)2, CCSD(T), among others), which account for electron correlation effects, perform very well for predicting the properties of many systems, including π-conjugated, but the associated computational cost is high. The known hierarchy of these methods allows for systematic improvement up to methods that can reach thermochemical accuracy, i.e., provide energies with errors smaller than 1 kcal/mol. One such method is the coupled cluster with explicit single and double excitations and perturbative triple excitations (CCSD(T)) with a complete basis set (CBS), abbreviated as CCSD(T)/CBS, which is nowadays considered the gold standard of QC.

DFT represents an alternative solution of the Schrödinger equation, which in principle can describe all physical effects within the framework of functionals of the electron density. Contrary to HF and semi-empirical methods, DFT includes in its formalism a complete description of both same- or opposite-spin electron correlation; historically there exist functionals for both exchange and correlation effects separately. The computational time for DFT calculations is particularly suited for most of wine pigments, offering a decent compromise between accuracy and computational effort compared to post-HF methods. These exchange-correlation functionals can be built upon the electronic density (and its gradient, and even its Laplacian) only, or the exchange part can be merged with a given percentage of HF-like exchange; the latter are called hybrid functionals (e.g., B3LYP, B3P86, PBE0) and perform satisfactorily at describing thermodynamics, kinetics, and optical properties of π-conjugated systems. However, these methods fail at describing non-covalent interactions at large (long-range) inter-

electronic distances. Approximate methods such as vdW-DF and DFT-D can largely include these interactions at a reasonable computational cost, making the full approach competitive enough to be successfully applied within the field. CT is also a challenging issue in theoretical chemistry, which can be assessed using range-separated hybrid (RSH) functionals (e.g., ωB97X and CAM-B3LYP) that (mathematically) split the particle-particle interaction operator into short- and long-range interactions. Scheme 1 summarizes the hierarchy of this wide array of methods.

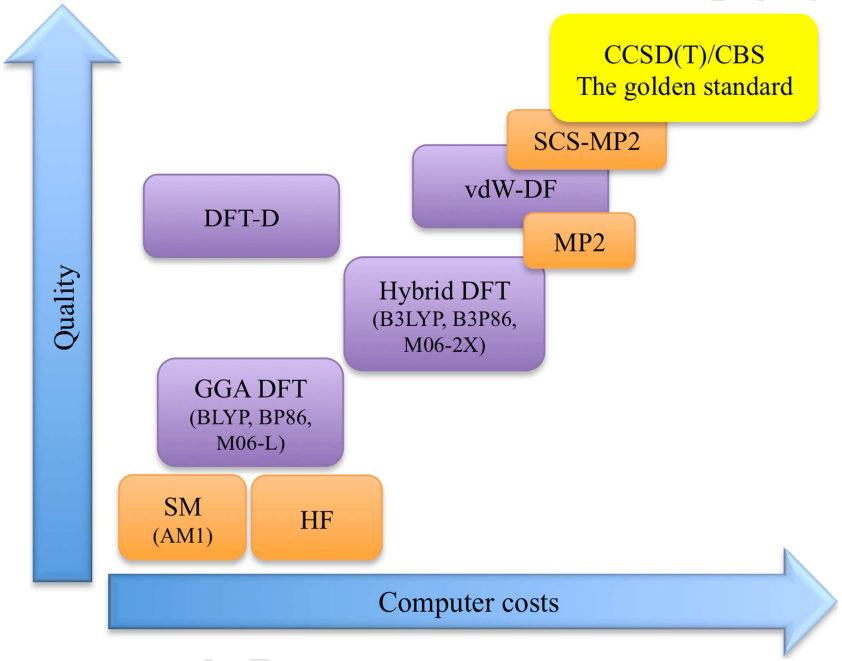

Scheme 1: Hierarchy of quantum methods to deal with π-conjugated systems and non-covalent interactions (H-bonding and π-stacking).

Mixed methodologies may also be used, i.e., optimizing at a certain level of theory and calculating electronic energies of ground state (GS) or excited state (ES) at a higher level of theory. The corresponding standard notation is *method1//method2*, in which *methods 1* and *2* are used for energy and optimization, respectively e.g., MP2/6-311+G(d,p)//B3LYP/6-31G(d).

Table S1. (a) Intramolecular and (b) solvent-solute averaged H-bond distances (d, Å) and their distribution ($D_{H\text{-}bond}$, %) over 100 ns MD simulation for each partner.

(a)

Partner	Donor	Acceptor	D (Å)	$D_{H\text{-}bond}$
Quercetin	O4	H5	2.66	98.6%
	O4	H3	2.62	28.9%
	O3'	H4'	2.74	10.9%
	O4'	H3'	2.75	1.5%
3-O-methylcyanidin	O3'	H4'	2.74	8.9%

(b)

Partner	Donor	Acceptor	d (Å)	$D_{H\text{-}bond}$
Quercetin	Water	H7	2.76	86%
	Water	H3'	2.77	83%
	Water	H4'	2.78	70%
	O4	Water	2.79	55%
	Water	H3	2.83	49%
	O3'	Water	2.82	45%
	O7	Water	2.84	42%
	O4'	Water	2.83	37%
	O5	Water	2.85	32%
	O3	Water	2.85	19%
	Water	H5	2.87	10%
3-O-methylcyanidin	Water	H3'	2.75	91.8%
	Water	H7	2.74	86.0%
	Water	H5	2.74	85.2%
	Water	H4'	2.77	74.0%
	O3'	Water	2.83	34.3%
	O7	Water	2.85	26.5%
	O4'	Water	2.85	21.2%
	O5	Water	2.86	16.7%
	O3	Water	2.87	2.6%